JAMA Otolaryngology–Head & Neck Surgery | Original Investigation

Fusion of Computed Tomography and PROPELLER Diffusion-Weighted Magnetic Resonance Imaging for the Detection and Localization of Middle Ear Cholesteatoma

Garrett D. Locketz, BSc; Peter M. M. C. Li, MD; Nancy J. Fischbein, MD; Samantha J. Holdsworth, PhD; Nikolas H. Blevins, MD

IMPORTANCE A method to optimize imaging of cholesteatoma by combining the strengths of available modalities will improve diagnostic accuracy and help to target treatment.

OBJECTIVE To assess whether fusing Periodically Rotated Overlapping Parallel Lines With Enhanced Reconstruction (PROPELLER) diffusion-weighted magnetic resonance imaging (DW-MRI) with corresponding temporal bone computed tomography (CT) images could increase cholesteatoma diagnostic and localization accuracy across 6 distinct anatomical regions of the temporal bone.

DESIGN, SETTING, AND PARTICIPANTS Case series and preliminary technology evaluation of adults with preoperative temporal bone CT and PROPELLER DW-MRI scans who underwent surgery for clinically suggested cholesteatoma at a tertiary academic hospital. When cholesteatoma was encountered surgically, the precise location was recorded in a diagram of the middle ear and mastoid. For each patient, the 3 image data sets (CT, PROPELLER DW-MRI, and CT-MRI fusion) were reviewed in random order for the presence or absence of cholesteatoma by an investigator blinded to operative findings.

MAIN OUTCOMES AND MEASURES If cholesteatoma was deemed present on review of each imaging modality, the location of the lesion was mapped presumptively. Image analysis was then compared with surgical findings.

RESULTS Twelve adults (5 women and 7 men; median [range] age, 45.5 [19-77] years) were included. The use of CT-MRI fusion had greater diagnostic sensitivity (0.88 vs 0.75), positive predictive value (0.88 vs 0.86), and negative predictive value (0.75 vs 0.60) than PROPELLER DW-MRI alone. Image fusion also showed increased overall localization accuracy when stratified across 6 distinct anatomical regions of the temporal bone (localization sensitivity and specificity, 0.76 and 0.98 for CT-MRI fusion vs 0.58 and 0.98 for PROPELLER DW-MRI). For PROPELLER DW-MRI, there were 15 true-positive, 45 true-negative, 1 false-positive, and 11 false-negative results; overall accuracy was 0.83. For CT-MRI fusion, there were 20 true-positive, 45 true-negative, 1 false-positive, and 6 false-negative results; overall accuracy was 0.90.

CONCLUSIONS AND RELEVANCE The poor anatomical spatial resolution of DW-MRI makes precise localization of cholesteatoma within the middle ear and mastoid a diagnostic challenge. This study suggests that the bony anatomic detail obtained via CT coupled with the excellent sensitivity and specificity of PROPELLER DW-MRI for cholesteatoma can improve both preoperative identification and localization of disease over DW-MRI alone.

Author Affiliations: Department of Otolaryngology–Head and Neck Surgery, Stanford University, Stanford, California (Locketz, Li, Fischbein, Blevins); Department of Radiology, Stanford University, Stanford, California (Fischbein, Holdsworth).

Corresponding Author: Nikolas H. Blevins, MD, Department of Otolaryngology–Head and Neck Surgery, Stanford University, 801 Welch Rd, Stanford, CA 94305 (nblevins@ohns.stanford.edu).

JAMA Otolaryngol Head Neck Surg. 2016;142(10):947-953. doi:10.1001/jamaoto.2016.1663
Published online July 14, 2016.

Computed tomography (CT) has traditionally been the imaging modality of choice for diagnosis and evaluation of clinically suspected cholesteatoma. Despite its excellent spatial resolution, high sensitivity, and precise delineation of key anatomical landmarks,[1] a limitation of CT is its low specificity for differentiating cholesteatoma from other soft tissue (granulation tissue, inflammation, cholesterol granuloma, or fibrosis) or from fluid in the middle ear or mastoid.[2] These soft tissues are present in 20% to 30% of previously operated ears, regardless of whether cholesteatoma is present.[3] Other studies have shown the sensitivity, specificity, and positive predictive value of CT in diagnosing residual and/or recurrent cholesteatoma to be only 42.9%, 48.3%, and 28.6%, respectively.[3,4] As a result, "second-look" surgical exploration remains the benchmark diagnostic modality for residual and/or recurrent cholesteatoma.

Because of its ability to help distinguish cholesteatoma from granulation tissue, diffusion-weighted magnetic resonance imaging (DW-MRI) has recently emerged as a promising tool for cholesteatoma diagnosis. It is particularly useful in cases of residual and/or recurrent disease, but also for initial diagnosis of congenital and acquired cholesteatoma in which otoscopic findings are equivocal.[1,5,6] Recently, several non–echo planar imaging (EPI)–based DW imaging (non-EPI DW-MRI) sequences have been evaluated in cholesteatoma diagnosis,[6-9] including HASTE (Half Fourier Acquisition Single Shot Turbo Spin Echo; Siemens) and PROPELLER (Periodically Rotated Overlapping Parallel Lines With Enhanced Reconstruction; General Electric). These non-EPI DW-MRI sequences can achieve a higher spatial resolution than routine EPI-based DW-MRI sequences and are sensitive to cholesteatomas as small as 2 to 3 mm.[3,5-7,9,10] These sequences also require shorter acquisition times and are less susceptible to airbone distortions than EPI DW-MRI, with PROPELLER being less susceptible to motion artifacts than other non-EPI DW-MRI sequences. A recent meta-analysis of the published literature found the overall sensitivity and specificity of non-EPI DW-MRI in detecting cholesteatoma to be 0.94 and 0.94, respectively, lending support to the notion that these sequences may reduce the need for second-look surgery.[6,7,11,12]

Nevertheless, precise localization of cholesteatoma within the middle ear and mastoid remains a challenge using DW-MRI (whether EPI or non-EPI), and CT remains the mainstay of preoperative planning given its bony anatomic detail. To address this issue of localization, we sought to assess whether localization accuracy could be increased by the fusion of PROPELLER DW-MRI with corresponding temporal bone CT images. We directly compared the diagnostic and localization accuracy of PROPELLER DW-MRI alone to that of CT-MRI fusion imaging, and stratified this accuracy across 6 distinct surgically relevant anatomical locations.

Key Points

Question Can the diagnosis and localization of middle ear cholesteatoma be improved by fusing PROPELLER diffusion-weighted magnetic resonance imaging (DW-MRI) with corresponding temporal bone computed tomography (CT)?

Findings In a case series of 12 adults with clinically suspected cholesteatoma, CT-MRI fusion increased diagnostic sensitivity and positive and negative predictive value compared with PROPELLER DW-MRI alone. Image fusion also showed increased overall localization accuracy across 6 distinct anatomical regions of the temporal bone.

Meaning The bony anatomic detail obtained via CT coupled with the excellent sensitivity and specificity of PROPELLER DW-MRI for cholesteatoma can improve both preoperative identification and localization of this condition over either modality alone.

Figure 1. Operative Diagram

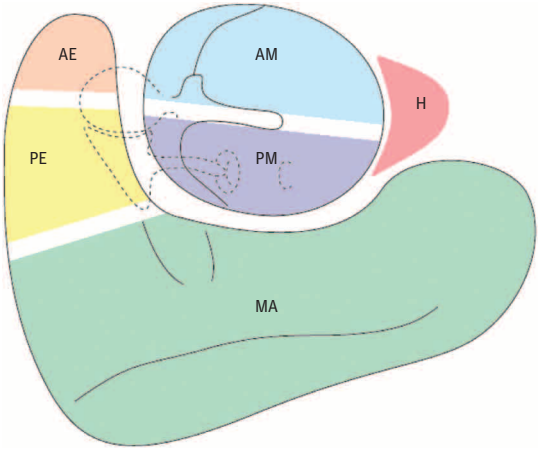

AE indicates anterior epitympanum; AM, anterior mesotympanum; H, hypotympanum; MA, mastoid/antrum; PE, posterior epitympanum; and PM, posterior mesotympanum.

Methods

This retrospective feasibility study was approved by the Stanford University Institutional Review Board. Informed consent was waived due to the retrospective nature of the study.

The following inclusion criteria were used: adults who underwent preoperative PROPELLER DW-MRI and CT scans with subsequent surgery by one of us (N.B.) for clinically suggested cholesteatoma. When cholesteatoma was encountered intraoperatively, the precise location was recorded on a diagram of the middle ear and mastoid (**Figure 1**). This diagram divides the mastoid and middle ear into 6 distinct surgically relevant locations, including the antrum/mastoid cavity, posterior epitympanum, anterior epitympanum, anterior mesotympanum, posterior mesotympanum, and hypotympanum. Data collected from patient medical records included patient age and sex, otologic history, dates of image acquisition, imaging techniques/protocols used, and time between MRI and surgery.

Computed Tomography Protocol

Computed tomography imaging was performed on either a Siemens Somatom Definition Dual Source CT scanner or a Gen-

Table 1. Patient Demographic Characteristics, Imaging Interpretation via Computed Tomography (CT), PROPELLER Diffusion-Weighted Magnetic Resonance Imaging (DW-MRI), and CT-MRI Fusion, and Operative Findings

Patient No./Sex	MRI to Surgery, d	CT			DW-MRI			CT-MRI Fusion			Surgery	
		Diagnosis	Location	Size, cm	Diagnosis	Location	Size, cm	Diagnosis	Location	Size, cm	Diagnosis	Location
1/F	6	Indeterminate	MA, PE, AE, AM, PM, H	2.2 × 0.8	No	...	...	No	...	...	No	...
2/M	2	Yes	PE, AE, AM, PM, H	0.7 × 0.7	Yes	MA, AE, AM	0.5 × 0.7	Yes	MA, PE, PM, H	0.7 × 9.7	Yes	MA, PE, AE, AM, PM, H
3/F	1	Indeterminate	H	0.2 × 0.3	No	...	...	No	...	...	No	...
4/M	3	Indeterminate	PE, PM	0.3 × 0.8	Yes	MA, PE	0.4 × 0.6	Yes	MA, PE	0.8 × 0.5	Yes	MA, PE, AM
5/M	30	Indeterminate	...	...	Yes	MA	0.3 × 0.5	Yes	MA	0.5 × 0.5	No	...
6/F	2	Indeterminate	AM, H	0.5 × 0.6	No	...	...	No	...	...	No	...
7/F	12	Yes	MA, PE, AE	1.0 × 2.5	Yes	MA, PE, AE	0.8 × 2.5	Yes	MA, PE, AE	0.9 × 2.5	Yes	MA, PE, AE
8/M	1	Yes	MA, PE, AE, AM, PM, H	1.9 × 0.9	Yes	MA, PE, AE, AM	1.0 × 2.2	Yes	MA, PE, AE, AM, PM, H	1.0 × 2.0	Yes	MA, PE, AE, AM, PM, H
9/M	16	Indeterminate	MA, PE, AE, AM, PM, H	1.5 × 2.5	Yes	MA, PE	1.2 × 1.4	Yes	MA, PE, AE	1.2 × 2.0	Yes	MA, PE, AE
10/F	1	Yes	MA, PE, AE, AM, PM, H	0.6 × 0.9	Yes	AE	0.4 × 0.5	Yes	AE	0.4 × 0.5	Yes	PE, AE
11/M	168	Indeterminate	...	...	No	...	...	No	...	...	Yes	PE
12/M	92	Indeterminate	PE	0.3 × 0.7	No	...	...	Yes	PE	0.2 × 0.3	Yes	PE, AE

Abbreviations: AE, anterior epitympanum; AM, anterior mesotympanum; ellipses, no pathology or negative result; H, hypotympanum; MA, mastoid/antrum; PE, posterior epitympanum; PM, posterior mesotympanum; PROPELLER, Periodically Rotated Overlapping Parallel Lines With Enhanced Reconstruction.

eral Electric VCT CT scanner, each with 64-slice capability. Images were acquired in a single acquisition using routine temporal bone protocols, with kV(peak), 140; mA, 170; and exposure time, 1 second. Imaging data were then reformatted into 0.5-mm slice thickness (Siemens) or 0.625-mm slice thickness (General Electric) and viewed with a display field of view of 10 cm in reconstructed axial, coronal, and sagittal planes.

PROPELLER DW-MRI Protocol

All patients underwent examinations with a 1.5T whole-body MRI unit (General Electric Excite) and an 8-channel head coil. The PROPELLER DW-MRI image parameters were repetition time/echo time, 6000 ms/113 ms; field of view, 24 cm; acquisition matrix, 256 × 256; echo train length, 20; number of averages, 1.5; scan time, 2:34 minutes. One non-DW image (b value = 0 s/mm^2) and 3 isotropic (*x, y, z*) DW images with b value of 1000 s/mm^2 were acquired, resulting in a scan time of 2:34 minutes.

CT-MRI Fusion Protocol

To fuse the imaging sequences, the CT and PROPELLER DW-MRI data were uploaded into Amira 4.0 (FEI), co-registered in 3 dimensions, cropped to size, and exported as individual CT and DW-MRI DICOM (Digital Imaging and Communications in Medicine) image stacks. These were individually imported into OsiriX, version 6.0.1 (OsiriX Imaging Software), overlaid on each other using the fusion protocol, and subsequently evaluated. The fusion process was performed by an otolaryngologic surgeon with minimal software experience, and required a mean of approximately 10 minutes per patient.

Imaging Interpretation

All imaging was prospectively evaluated by a specialist in head and neck radiology (N.J.F.). For each patient, the 3 image data sets (CT, PROPELLER DW-MRI, and CT-MRI fusion) were assigned a random number and reviewed in random order for the presence or absence of cholesteatoma by a radiologist (N.J.F.) blinded to the knowledge of operative findings. If deemed to be present, the cholesteatoma was localized presumptively on each imaging modality. Localization data were not recorded for indeterminate soft tissue that was not suspicious for cholesteatoma.

Statistical Analysis

The positive and negative predictive values were calculated in a standard manner for each group. Positive predictive value indicates the probability that a positive radiologic result correctly predicts the presence of cholesteatoma (number of true positives for cholesteatoma found at surgery/total number of positive radiologic results). The negative predictive value indicates the probability that a negative radiologic result correctly predicts the absence of cholesteatoma (number of true negatives for cholesteatoma confirmed at surgery/total number of negative radiologic results).

Results

Patients

Twelve adults, 5 women and 7 men, aged 19 to 77 years (median, 45.5 years) with clinically suspected cholesteatoma and

Table 2. Surgical, Diffusion-Weighted Magnetic Resonance Imaging (DW-MRI), and Computed Tomography (CT) Findings Across Patients and Anatomic Locations

	Patient No.												
Anatomic Location	1	2	3	4	5	6	7	8	9	10	11	12	Accuracy
PROPELLER DW-MRI[a]													
Mastoid/antrum		R+, S+		R+, S+	R+		R+, S+	R+, S+	R+, S+				0.92
Posterior mesotympanum		S+						S+					0.83
Anterior epitympanum		R+, S+					R+, S+	R+, S+	S+	R+, S+		S+	0.83
Posterior epitympanum		S+		R+, S+			R+, S+	R+, S+	R+, S+	S+	S+	S+	0.67
Anterior mesotympanum		R+, S+		S+				R+, S+					0.92
Hypotympanum		S+						S+					0.83
Accuracy	1.0	0.5	1.0	0.83	0.83	1.0	1.0	0.67	0.83	0.83	0.83	0.67	
CT-MRI Fusion[b]													
Mastoid/antrum		R+, S+		R+, S+	R+		R+, S+	R+, S+	R+, S+				0.92
Posterior mesotympanum		R+, S+						R+, S+					1.0
Anterior epitympanum		S+					R+, S+	R+, S+	R+, S+	R+, S+		S+	0.83
Posterior epitympanum		R+, S+		R+, S+			R+, S+	R+, S+	R+, S+	S+	S+	R+, S+	0.83
Anterior mesotympanum		S+		S+				R+, S+					0.83
Hypotympanum		R+, S+						R+, S+					1.0
Accuracy	1.0	0.67	1.0	0.83	0.83	1.0	1.0	1.0	1.0	0.83	0.83	0.83	

Abbreviations: PROPELLER, Periodically Rotated Overlapping Parallel Lines With Enhanced Reconstruction; R+, radiographic disease; S+, surgical disease.

[a] For PROPELLER DW-MRI, localization sensitivity and specificity were 0.58 and 0.98, respectively. There were 15 true-positive, 45 true-negative, 1 false-positive, and 11 false-negative results; overall accuracy was 0.83.

[b] For CT-MRI fusion, localization sensitivity and specificity were 0.76 and 0.98, respectively. There were 20 true-positive, 45 true-negative, 1 false-positive, and 6 false-negative results; overall accuracy was 0.90.

subsequent surgery by one of us (N.B.) were selected (**Table 1**). Four patients had a clinical history of cholesteatoma with 1 or more previous attempts at removal. In 3 cases, previous surgery involved unilateral canal wall-up mastoidectomy, and in 1 case, a partial canal wall-down mastoidectomy was required.

Cholesteatoma Diagnosis

Eight of 12 cases were positive for cholesteatoma on surgery; 6 were primary and 2 were residual and/or recurrent cases. The median time interval between MRI imaging and surgery was 3 days (range, 1-168 days). Computed tomographic examination was deemed positive for cholesteatoma in 4 cases and indeterminate in 8 patients (including all 4 residual and/or recurrent cases) due to nonspecific opacification of the middle ear spaces without evidence of bony erosion. Preoperative PROPELLER DW-MRI correctly predicted the presence of cholesteatoma in 6 of 8 patients (0.75 sensitivity), with both false-negative results interpreted as indeterminate on CT imaging. One false-positive result was recorded with PROPELLER DW-MRI (specificity of 0.75), yielding an overall positive and negative predictive value of 0.86 and 0.60, respectively. When preoperative PROPELLER DW-MRI was fused with CT, 1 false-negative result was converted to a true-positive result, yielding an overall sensitivity, specificity, and positive and negative predictive value of 0.88, 0.75, 0.88, and 0.75, respectively, for the CT-MRI fusion.

Cholesteatoma Localization

When localization was stratified across the 6 distinct anatomical areas, the overall accuracy of PROPELLER DW-MRI was 83% (range, 67%-92%) (**Table 2**). Accuracy calculations took into account areas positively identified for disease (true-positive results) and areas correctly identified as free of disease (true-negative results). The most accurate locations were the mastoid/antrum (92%) and anterior mesotympanum (92%), and least accurate was the posterior epitympanum (67%). When each individual anatomical location was examined independently, PROPELLER DW-MRI showed an overall localization sensitivity of 58% and overall localization specificity of 98%.

When PROPELLER DW-MRI sequences were fused with their corresponding CT images, the MRI-hyperintense cholesteatoma became situated within the bony anatomical confines of the CT, increasing overall localization accuracy to 90%. The most accurate locations were the posterior mesotympanum (100%) and hypotympanum (100%), and least accurate were anterior epitympanum (83%), posterior epitympanum (83%), and anterior mesotympanum (83%). When individual anatomical locations were examined independently across patients, CT-MRI fusion showed an overall localization sensitivity of 76% and overall localization specificity of 98%. Only 1 false-positive localization was recorded on both PROPELLER DW-MRI and CT-MRI fusion (mastoid/antrum), and thus all other locations had 100% specificity.

Discussion

Currently, no single imaging modality is best suited for detection and precise localization of cholesteatoma, whether congenital, acquired, residual, or recurrent. Historically, CT has been most commonly used, and cholesteatoma is strongly suggested when a localized soft-tissue lesion is seen adjacent to eroded bone. However, using CT

Figure 2. Computed Tomographic (CT) Scan, PROPELLER Diffusion-Weighted Magnetic Resonance Image (DW-MRI), and Fused Images for a Man With High-Frequency Sensorineural Hearing Loss and Tinnitus

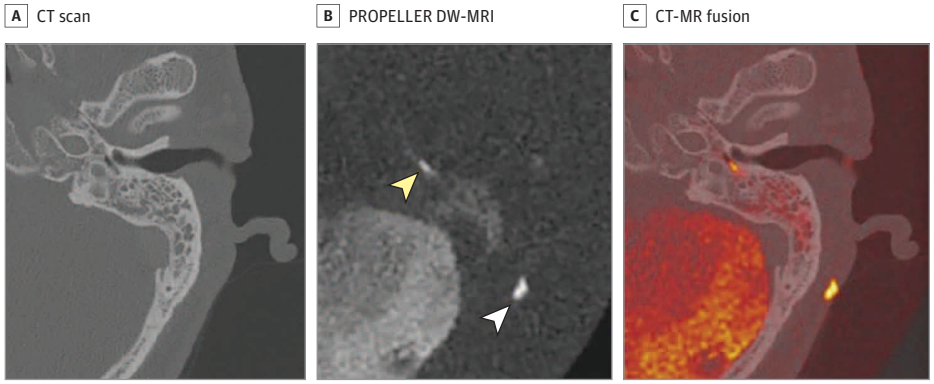

A, The CT scan shows nonspecific opacification of mastoid air cells and hypotympanum. B, PROPELLER DW-MRI shows foci of high intensity in the expected region of the hypotympanum (yellow arrowhead), and a second focus of uncertain location posteriorly (white arrowhead). C, The CT-MRI fusion clearly localizes both foci. The hypotympanic signal was related to a cholesteatoma, whereas the extratemporal focus was presumed to be a clinically insignificant lymph node. This illustrates CT-MRI fusion's capacity for both improved diagnostic and avoidance of a false-positive result seen on MRI alone.

Figure 3. Computed Tomographic (CT) Scan, PROPELLER Diffusion-Weighted Magnetic Resonance Image (DW-MRI), and Fused Images for a Man With Progressive Hearing Loss

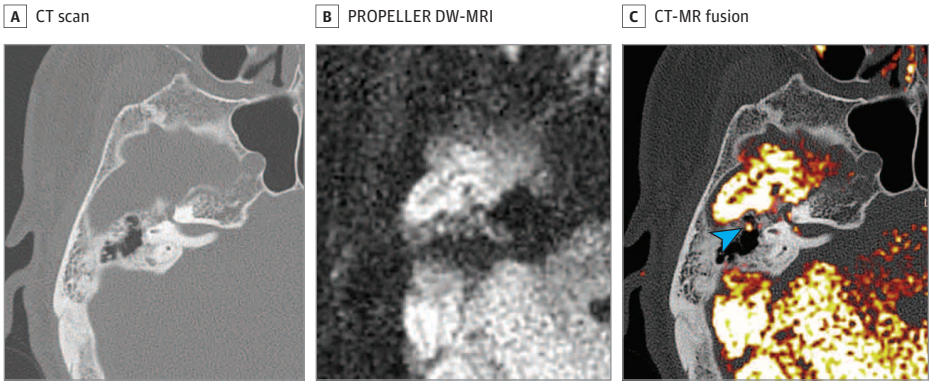

A, The CT scan shows nonspecific opacification of the anterior epitympanum and mastoid air cells. B, PROPELLER DW-MRI shows multiple heterogeneous nonspecific signal foci through the middle ear and epitympanum. C, The CT-MRI fusion demonstrates a focus of hyperintensity in the anterior epitympanum, which was confirmed to be cholesteatoma at the time of surgery (arrowhead).

imaging to differentiate cholesteatoma from granulation tissue in an opacified mastoid is substantially more challenging. In our patient population, CT had indeterminate results in 8 cases, and its overall localization accuracy was only 62.5% when stratified across the 6 distinct anatomical locations.

Although initially developed for detecting cerebral infarction, DW-MRI techniques have recently been applied to diagnosis of cholesteatoma. In DW-MRI, the image signal intensity reflects the rate of water diffusion within the imaged tissue, whereby a hyperintense signal corresponds to a situation in which the motion of water molecules is reduced or "restricted." In cerebral infarction, areas of acute ischemia show reduced diffusion of water molecules relative to normal areas, whereas in cholesteatoma, the motion of water is restricted by the tightly organized cholesteatoma matrix. Therefore, DW sequences show cholesteatoma to be markedly bright relative to other commonly encountered materials within the temporal bone, which increases its diagnostic sensitivity over other MRI sequences. The most widely used DW-MRI acquisition is the EPI technique, although an important limitation to its use in cholesteatoma diagnosis is its susceptibility to distortions at air-bone and bone-tissue interfaces, which are numerous within the temporal bone and skull base and may lead to inaccurate diagnosis.[8-10] To address this lack of specificity, non-EPI DW-MRI sequences (including HASTE and PROPELLER) can achieve a higher spatial resolution than traditional EPI DW-MRI and are thus less susceptible to air-bone and bone-tissue distortions. As such, the PROPELLER DW-MRI technique was selected for use in our study. Consistent with previous literature, we found PROPELLER DW-MRI alone to be more accurate than CT in detecting cholesteatoma in our patients.

As can be seen in **Figure 2** and **Figure 3**, when CT images are superimposed and fused with their corresponding PROPELLER DW-MRI images, the MR-hyperintense cholesteatoma becomes situated within the bony anatomical details of

the CT, improving both preoperative identification and localization of disease over each modality alone. Figure 2 displays imaging of a man in his 50s with 15 years of high-frequency sensorineural hearing loss and progressive pulsatile tinnitus on the left side. Temporal bone CT scan (Figure 2A) demonstrates nonspecific opacification of mastoid air cells and nonspecific soft tissue within the hypotympanum, adjacent to a thickened tympanic membrane. PROPELLER DW-MRI (Figure 2B) demonstrates foci of high signal intensity suggestive of cholesteatoma in both the middle ear (yellow arrowhead), as well as posteriorly, possibly within the mastoid (white arrowhead). Computed tomography–MRI fusion imaging (Figure 2C) clearly localizes the more anterior focus of high signal to the posteroinferior hypotympanum, while the more posterior focus lies outside the mastoid in the soft tissues, likely representing a reactive lymph node. This case illustrates the potential for the additional anatomic information gained on CT to increase the specificity of MRI findings. Figure 3 displays imaging of a man in his 50s with a 5-year history of progressive hearing loss on the right side. Microscopic examination showed a superior retraction pocket with debris, suggestive of an epitympanic cholesteatoma. A temporal bone CT scan (Figure 3A) revealed subtle and nonspecific opacification of the anterior epitympanum and adjacent mastoid air cells, and PROPELLER DW-MRI (Figure 3B) showed multiple nonspecific foci of signal intensity similar to that of brain parenchyma. One or more of these foci were potentially concerning for cholesteatoma; however, their precise location and therefore clinical significance was unclear given the lack of anatomic detail via PROPELLER DW-MRI. Subsequent CT-MRI fusion imaging localized the area of highest MRI signal to those areas of the anterior epitympanic soft tissue most concerning for cholesteatoma on CT (Figure 3C), which was consistent with surgical findings. This case illustrates the synergistic nature of these 2 modalities to aid in identifying and localizing cholesteatoma. Surgical findings and imaging analysis for all patients are listed in Table 1.

Despite its advantages, CT-MRI fusion itself does not resolve the potential for both false-positive and false-negative results encountered with non-EPI DW MRI alone. In DW-MRI, each image voxel has a signal intensity that reflects the rate of water diffusion within the tissue included in the voxel, and a hyperintense signal corresponds to a situation in which the motion of water molecules is reduced or "restricted." The DW-MRI techniques were initially and continue to be routinely used in the diagnosis of cerebral infarction, as areas of acute ischemia (cell swelling of cytotoxic edema) show reduced diffusion of water molecules relative to normal areas. Typically, the most widely used DW-MRI acquisition is the EPI technique due to its high imaging speed.[13] Although EPI DW-MRI is relatively rapid and does not require the injection of contrast material, an important limitation to its use in cholesteatoma diagnosis is its susceptibility to distortions at air-bone and bone-tissue interfaces, which are numerous within the temporal bone and skull-base and may lead to inaccurate diagnosis.[10,14,15] Furthermore, the exact cause of the hyperintensity seen on DW-MRI when imaging cholesteatoma is still open to debate. Although restricted diffusion of water molecule motion within a cholesteatoma clearly plays a role in generating high signal intensity on DWI, a "T2 shine-through" effect has been proposed as 1 possible explanation for the high signal, referring to the hyperintense signal observed in tissues that have prolonged T2 relaxation.[7,10] In addition to cholesteatoma, tissues exhibiting prolonged T2 relaxation potentially include bone powder,[14] other keratin-containing substances such as cerumen,[7,15] Silastic sheets,[16] and cartilage grafts[5]—all of which have the potential to elicit false-positive diagnoses with DW-MRI (both EPI and non-EPI), and thus also with CT-MRI fusion. In the present study, 1 false-positive result was recorded with PROPELLER DW-MRI (specificity of 0.75), which may be attributable to a tragal cartilage graft used in previous surgery.[5,7]

In addition, the diagnostic threshold of 2 to 3 mm for cholesteatoma diagnosis remains a limitation of CT-MRI fusion and can lead to false-negative results as with PROPELLER DW-MRI alone. Two false-negative results were recorded with CT-MRI fusion in the present series, 1 of which was a reoperative patient with chronic ear disease who was found at surgery to have a residual cholesteatoma of less than 3 mm in size. The other patient with a false-negative result was found on PROPELLER DW-MRI to have a 2 × 3-mm area of intermediate signal intensity within the epitympanum, concerning for cholesteatoma but without convincing reduced diffusion on the PROPELLER DW-MRI sequence. This patient's cholesteatoma may too have been below the diagnostic threshold for non-EPI DW-MRI, or there may have been some alteration in tissue composition that made it less diffusion restricting and hence more difficult to detect. It is also worth noting that, in this patient, the interval between original PROPELLER DW-MRI image acquisition and surgery was 168 days, which may have allowed time for the cholesteatoma to change in size over the interim.

Recently, Plouin-Gaudon et al[15] investigated CT-MRI fusion for cholesteatoma diagnosis in pediatric patients. Although the authors did not directly compare the precise localization accuracy of DW-MRI to that of CT-MRI fusion, 3 of their 10 patients had their surgical approach modified on the basis of CT-MRI fusion results. These results are supported by our present series, in that CT-MRI fusion provided a more accurate depiction of cholesteatoma location, which may potentially influence surgical approach. Furthermore, the finding of 1 false-negative result on PROPELLER DW-MRI converting to a true-positive result on CT-MRI fusion supports the notion that this technique may influence the initial decision of when to operate.

Despite its limited sample size, our study demonstrates the feasibility of the CT-MRI fusion technique and offers promising preliminary results in favor of increased localization accuracy without any increase in false-positive or false-negative results. Nevertheless, the relative increase in accuracy must be weighed against the additional cost of acquiring MRI imaging, especially when there is clear clinical evidence of cholesteatoma. Given these preliminary results, the argument could be made for the use of non-EPI DW-MRI as the primary modality for cholesteatoma detection and postoperative surveillance, followed by CT and CT-MRI fusion in cases in which non-EPI DW-MRI has positive results. Such an approach may

both be effective and serve to limit radiation exposure. Regardless of which modality is obtained first, it is worth noting that the interpretation of CT-MRI fusion images should be considered a new process and is thus subject to a learning curve. Furthermore, variation exists among centers regarding imaging systems and DW-MRI protocols, and it is yet unclear which are best for creating fusion images. Nevertheless, with the growing use of non-EPI DW-MRI instead of second-look surgery to rule out recurrent and/or residual cholesteatoma,[5,6,11] CT-MRI fusion may become increasingly useful because both modalities may already be acquired in select patients, and fusion techniques can be rapid to accomplish. Our study serves as a preliminary evaluation of the feasibility of the fusion technique presented. Further investigation into CT-MRI fusion with sample sizes sufficient for definitive statistical interpretation will be needed to establish the efficacy of this approach.

Conclusions

Computed tomography provides excellent spatial resolution of key anatomical landmarks and provides high sensitivity for diagnosing cholesteatoma. Nevertheless, CT is nonspecific, and its inability to differentiate cholesteatoma from other soft tissues makes its utility in cholesteatoma localization limited. PROPELLER DW-MRI has recently emerged as a more specific imaging tool for cholesteatoma diagnosis, but it is limited by relatively poor anatomical spatial resolution, making precise localization of disease within the middle ear or mastoid a diagnostic challenge. Our results suggest that the tissue-specific diagnostic accuracy of PROPELLER DW-MRI fused with the bony anatomic detail obtained via CT improves cholesteatoma diagnosis and localization beyond either modality alone.

ARTICLE INFORMATION

Accepted for Publication: May 13, 2016.

Published Online: July 14, 2016. doi:10.1001/jamaoto.2016.1663.

Author Contributions: Mr Locketz had full access to all of the data in the study and takes responsibility for the integrity of the data and the accuracy of the data analysis.
Study concept and design: Locketz, Li, Fischbein, Blevins.
Acquisition, analysis, or interpretation of data: All authors.
Drafting of the manuscript: Locketz, Li, Fischbein, Blevins.
Critical revision of the manuscript for important intellectual content: Li, Fischbein, Holdsworth, Blevins.
Statistical analysis: Li, Blevins.
Administrative, technical, or material support: Li, Holdsworth, Blevins.
Study supervision: Locketz, Li, Fischbein, Blevins.

Conflict of Interest Disclosures: All authors have completed and submitted the ICMJE Form for Disclosure of Potential Conflicts of Interest and none were reported.

Previous Presentation: This study was presented at the American Academy of Otolaryngology–Head and Neck Surgery Annual Meeting; September 27-30, 2015; Dallas, Texas.

REFERENCES

1. De Foer B, Vercruysse JP, Pilet B, et al. Single-shot, turbo spin-echo, diffusion-weighted imaging versus spin-echo-planar, diffusion-weighted imaging in the detection of acquired middle ear cholesteatoma. *AJNR Am J Neuroradiol*. 2006;27(7):1480-1482.

2. Williams MT, Ayache D. Imaging of the postoperative middle ear. *Eur Radiol*. 2004;14(3):482-495.

3. De Foer B, Vercruysse JP, Pouillon M, Somers T, Casselman JW, Offeciers E. Value of high-resolution computed tomography and magnetic resonance imaging in the detection of residual cholesteatomas in primary bony obliterated mastoids. *Am J Otolaryngol*. 2007;28(4):230-234.

4. Tierney PA, Pracy P, Blaney SPA, Bowdler DA. An assessment of the value of the preoperative computed tomography scans prior to otoendoscopic 'second look' in intact canal wall mastoid surgery. *Clin Otolaryngol Allied Sci*. 1999;24(4):274-276.

5. Migirov L, Wolf M, Greenberg G, Eyal A. Non-EPI DW MRI in planning the surgical approach to primary and recurrent cholesteatoma. *Otol Neurotol*. 2014;35(1):121-125.

6. Li PMMC, Linos E, Gurgel RK, Fischbein NJ, Blevins NH. Evaluating the utility of non-echo-planar diffusion-weighted imaging in the preoperative evaluation of cholesteatoma: a meta-analysis. *Laryngoscope*. 2013;123(5):1247-1250.

7. Jindal M, Riskalla A, Jiang D, Connor S, O'Connor AF. A systematic review of diffusion-weighted magnetic resonance imaging in the assessment of postoperative cholesteatoma. *Otol Neurotol*. 2011;32(8):1243-1249.

8. De Foer B, Vercruysse JP, Bernaerts A, et al. The value of single-shot turbo spin-echo diffusion-weighted MRI imaging in the detection of middle ear cholesteatoma. *Neuroradiology*. 2007;49(10):841-848.

9. Lehmann P, Saliou G, Brochart C, et al. 3T MRI imaging of postoperative recurrent middle ear cholesteatomas: value of periodically rotated overlapping parallel lines with enhanced reconstruction diffusion-weighted MRI imaging. *AJNR Am J Neuroradiol*. 2009;30(2):423-427.

10. Baráth K, Huber AM, Stämpfli P, Varga Z, Kollias S. Neuroradiology of cholesteatomas. *AJNR Am J Neuroradiol*. 2011;32(2):221-229.

11. Migirov L, Tal S, Eyal A, Kronenberg J. MRI, not CT, to rule out recurrent cholesteatoma and avoid unnecessary second-look mastoidectomy. *Isr Med Assoc J*. 2009;11(3):144-146.

12. Rajan GP, Ambett R, Wun L, et al. Preliminary outcomes of cholesteatoma screening in children using non-echo-planar diffusion-weighted magnetic resonance imaging. *Int J Pediatr Otorhinolaryngol*. 2010;74(3):297-301.

13. Schwartz KM, Lane JI, Bolster BD Jr, Neff BA. The utility of diffusion-weighted imaging for cholesteatoma evaluation. *AJNR Am J Neuroradiol*. 2011;32(3):430-436.

14. Dubrulle F, Souillard R, Chechin D, Vaneecloo FM, Desaulty A, Vincent C. Diffusion-weighted MRI imaging sequence in the detection of postoperative recurrent cholesteatoma. *Radiology*. 2006;238(2):604-610.

15. Plouin-Gaudon I, Bossard D, Ayari-Khalfallah S, Froehlich P. Fusion of MRIs and CT scans for surgical treatment of cholesteatoma of the middle ear in children. *Arch Otolaryngol Head Neck Surg*. 2010;136(9):878-883.

16. Venail F, Bonafe A, Poirrier V, Mondain M, Uziel A. Comparison of echo-planar diffusion-weighted imaging and delayed postcontrast T1-weighted MRI imaging for the detection of residual cholesteatoma. *AJNR Am J Neuroradiol*. 2008;29(7):1363-1368.